Available online at **www.joac.info**

ISSN: 2278-1862

Journal of Applicable Chemistry

2018, 7 (2):343-352

(International Peer Reviewed Journal)

Macrocycle Adsorbed Hybrid Nanoparticles for Preconcentration and Atomic Absorption Spectrophotometric Estimation of Zinc from Acid Leached Rodenticide

Kundan C. Tayade, Sopan T. Ingle, Sanjay. B. Attarde*

School of Environmental and Earth Sciences, North Maharashtra University, Jalgaon-425001, **INDIA**
Email: sb.attarde@yahoo.co.in

Accepted on 6th February, 2018

ABSTRACT

*Hybrid nanoparticles (HNPs) were designed by adsorbing a newer serendipitous preorganized macrocyclic motif (**L**) on Fe_3O_4@SiO_2 distorted hexagonal and cubic nanoparticles. These magnetic HNPs are tested for efficiency of Zn(II) metal ion extraction. Simultaneously, Zn(II) ion is estimated using flame atomic absorption spectroscopy. This method is validated with acid leached commercial rodenticide sample. The recovery from HNPs was 98.70 % with relative standard deviation of ±2.56 %. Also, the rodenticide samples were analyzed in triplicate with quantitative recovery of 100.00±0.36 % without any matrix interference. The parameters affecting on the extraction efficiency viz. pH, initial concentration of Zn(II) ions and reusability of the reagent were studied. The effect of altering analyte concentrations was screened with basic adsorption models such as Langmuir, Freundlich and Temkin isotherms. The key HNPs were successfully applied for preconcentration of Zn(II) ions in real sample (rodenticide residue) analysis without bare matrix interference.*

Graphical Abstract

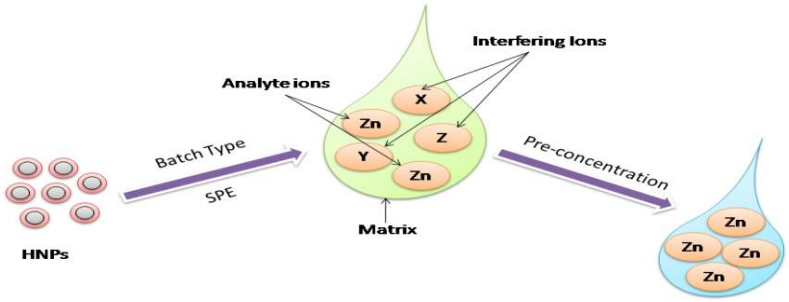

Highlights:

- Development of new HNPs as quantitative Solid Phase Extractor for enrichment of Zn(II) ions.
- Detailed exploration on sorption study and interpretation of equilibrium isotherms.

Validation of developed method by analyzing real sample of rodenticide without matrix interference.

Keywords: Hybrid Nanoparticles, Zn(II) ion extraction, Rodenticide analysis, AAS.

INTRODUCTION

Diverse range of promising applications of macrocycle doped HNPs like sensing [1], molecular switches [2], photocatalytic degradation [3], excellent extractants toward heavy metal ions [4] and pesticide residues [5], etc., have been reported. Albeit, considering doping of macrocyclic on nanoparticles, the majority of the HNPs are designed with derivatives of calixarenes [6]. Thus, the HNPs are smart materials with a myriad of applications [7]. Pristine Fe_3O_4 nanoparticles require modification (Fig. 1)[8-12] and a range of surface modification approaches such as, click chemistry, silica shell, gold shell, catechol coordination, etc. (Fig. 2) are used [13-20].

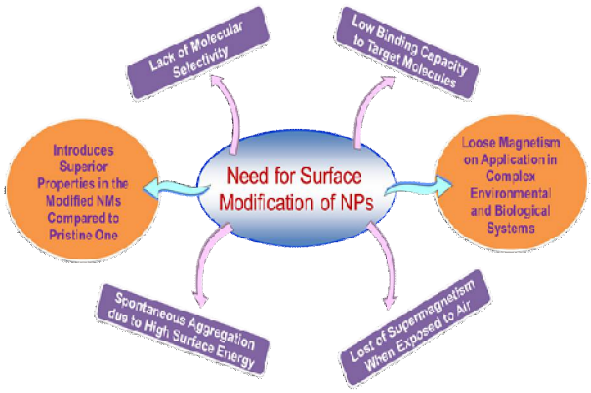

Figure 1. Key points indexing the need of modification of pristine nanoparticles

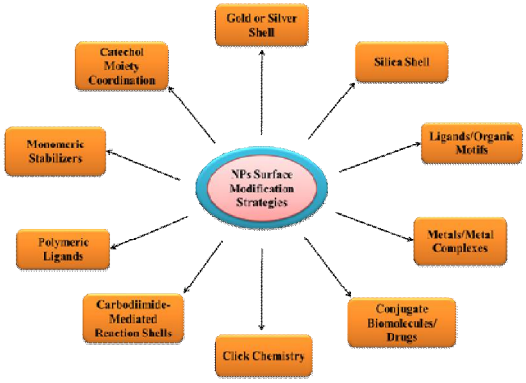

Figure 2. Representative strategies used for surface modification of nanoparticles

Literature reports revealed that, silica shell grafting is meticulously used to avoid loss of magnetism and the resultant mesoporous silica coated magnetic materials can be used as potential sorbents. But, it is found that these silica coated nanoparticles have imperfect adsorption capacity, rendering them unselective [21].

The perilous effects of heavy metal ions make it essential to keep check on their ever-increasing concentration, n harming flora and fauna [22]. In the present work, we have synthesized the HNPs by adsorbing a synthesized macrocyclic compound on silica coated Fe_3O_4 nanoparticles and used for Zn(II) ion extraction and estimation by FAAS.

MATERIALS AND METHODS

Anhydrous Ferric chloride ($FeCl_3$), Ferrous Chloride ($FeCl_2.4H_2O$) and liquor ammonia were procured from Sigma Aldrich, India. Tetra Ethyl Ortho Silicate (TEOS), glycerol, anhydrous ethanol, methanol and acetonitrile were obtained from Arcos Organics, Germany. High purity MILI-Q water was used throughout the study. The metal ion concentrations were measured by Atomic Absorption Spectrophotometer, Thermo Fisher, AAS-303.

Synthesis of HNPs: A solution of one mole *N*1-(2-aminoethyl) ethane-1,2-diamine (1.09 g; 10 mmol) and one mole of 1,4-diisocyanatobenzene (2.44 g; 20 mmol) in dry and degassed acetone (50 mL), was charged in a vessel. The mixture was stirred for 30 h, after which L was separated as whitish pale yellow colored powder which was washed with chloroform and ethanol.

Supermagnetic Fe_3O_4 NCs were synthesized by charging, anhydrous $FeCl_3$ (6.488 g; 40 mmol) and $FeCl_2.4H_2O$ (3.976 g; 20 mmol) in 200 mL degassed deionised water, in a three-necked vessel placed in an oil bath and heated to attain a constant temperature of 358 K, with stirring under nitrogen. Then 50 mL of liquor ammonia was added to the reaction mixture and then orange colored reaction mixture turned black. Consequently, the Fe_3O_4 magnetic nanostructures were washed several times with water, twice with sodium chloride solution (20 mM L^{-1}) and again with water. From the above solution, 20

mL volume was taken in a beaker and the NCs were allowed to settle with the help of a strong permanent magnet kept at the bottom of the container. Afterwards, the NCs get settled down, the supernatant liquid was discarded followed by addition of 10 % aqueous emulsion of TEOS (80 mL), followed by glycerol (60 mL). The pH of the resultant mixture was adjusted to 4.6, using acetic acid and ammonia. This stirring reaction mixture was charged in a two-necked flask and heated on a mantle for 2 hours at 363 K under nitrogen atmosphere. After two hours, a brown colored suspension obtained which indicates the silica core shell formation ($Fe_3O_4@SiO_2$). Afterwards, $Fe_3O_4@SiO_2$ colloids were washed with centrifugation/dispersion cycles in ethanol. A mixture of $Fe_3O_4@SiO_2$ and 0.05 % solution (100 mL) of L prepared in acetonitrile was ultrasonicated for 1 h at an ambient temperature and the solvent was evaporated. This footstep accomplished immobilization of L on $Fe_3O_4@SiO_2$ and the resultant hybrids ($Fe_3O_4@SiO_2@L$) were washed with several centrifugation/dispersion cycles in water. The washed NCs were dried into powder at an ambient temperature under vacuum [23-28].

Optimization of pH for Solid Phase Extraction of Zn(II) Ions: Literature review reveals that at pH range of 2-9 the Zn extract contains Zn^{2+} and Zn OH^+ ions which can be simply extracted. However, at the elevated pH the Zn(II) ions precipitate out as $Zn(OH)_2$ [29]. Furthermore, it is also revealed that in highly acidic ($pH \leq 2$) media barely small quantity of Zn(II) ion gets extracted which might be reunited to the high concentration of H^+ ions on the adsorbent surface. These ions may interfere sorption of analyte Zn(II) ions on adsorbent by adhering the active sites [30]. For confirming the extraction efficiency of HNPs, in a batch mode of solid phase extraction, 25 mg of the HNPs were conditioned for 1 h at different pH ranging from 3 to 10, obtained with dilute solution of hydrochloric acid (HCl) and ammonia (NH_3). Thus, consequently for further experimentation the optimized pH range 3 to 10 was selected. The nanoparticles were settled down with a magnet and the standard aqueous solutions of $ZnSO_4$ prepared in 1 M HNO_3 were used for the subsequent study. In addition, to these conditioned HNPs, 1 mL of 20 ppm solution of Zn(II) was added. Prior to adding this mixture to the conditioned HNPs, their pH values were readjusted to the desired pH values with the same acid and base. The sorbent HNPs along with the mixture of metal ions and desired pH solutions were sonicated for 1h. Thereafter, the HNPs were settled with magnet. Furthermore, the aqueous phase was decanted, followed by addition of 1M HCl (10 mL, stripping phase) to Zn(II) ion adsorbed HNPs, which was further sonicated for 40 minutes. This solution causes desorption of Zn(II) ions from the surface of sorbent. This solution was heated almost to dryness and finally diluted to 10 mL with 1 M nitric acid (HNO_3). For preparing the stripping blank 10 mL of 1 M HCl was evaporated by heating virtually to dryness and further the solution was diluted to 10 mL with 1 M HNO_3. For preparing the stripping standard, the mixture of 1 mL of 20 ppm solution of Zn(II) ion and 10 mL solution of 1M HCl was prepared in triplicate, heated approximately to dryness and diluted to 10 mL with 1M HNO_3. All these solutions were further analyzed by Atomic Absorption Spectrometer (AAS) for monitoring the concentration of Zn(II) ions.

Effect of Increasing Concentration on the Extraction: The effect of concentration on the extraction amount by the fixed quantity of sorbent was evaluated at the optimized pH. A series of standard solutions of Zn(II) ions were prepared ranging from 0.4 to 400 ppm, in triplicate. The concentrations of these prepared solutions were measured by AAS and their average was taken. Also, different basic mathematical models were applied to study the effect of rising concentration of Zn(II) metal ions on extraction by HNPs. After desorption of the extracted Zn(II) ions their concentrations were estimated by AAS.

Matrix Effect: To study the matrix effect with HNPs, rodenticide residues having approximately 3-4.5 % zinc phosphide (Zn_3P_2) per 100 g were analyzed. The Zn_3P_2 residue was mixed with 20 mL of propylene glycol followed by ultrasonication for 30 min and thorough mixing on a rotamixer for 10 min. The acid solution was added to it to hydrolyze propylene glycol. The solution was diluted to 100 mL by water and used as stock solution of rodenticide sample. Thus, the Zn_3P_2 solution was prepared by slender modification in the procedure mentioned in the literature to tackle the solubility and for

avoiding the generation of poisonous gas phosphine by direct treatment of Zn_3P_2 solution with acids [31]. 1 mL of stock solution of rodenticide sample was subjected to extraction by adjusting its pH to 2.7 with 0.25 g of HNPs. Then, the extracted zinc was stripped with 10 mL of 1 M HCl. To calculate the recovery with respect to rodenticide samples, sample solutions were analyzed by AAS and found to be 2.75, 2.78, 2.76 ppm with respect to concentration of Zn(II) ions for the triplicate samples. The recovery from HNPs was found 98.70 % with relative standard deviation of ±2.56 %. Also, the rodenticide samples were analyzed in triplicate with quantitative recovery of 100.00±0.36 % without any matrix interference.

RESULTS AND DISCUSSION

pH Optimization for Zn(II) Ion Extraction: The key factor affecting the sorption capacity of analyte on sorbent is pH. The extraction efficiency of Zn(II) ions on HNPs at various pH values in the range 3-10 was studied. The results of the extraction of Zn(II) on HNPs (Fig. 3) shows that maximum extraction takes place at pH 3. The Zn(II) extraction was screened in the pH range 3-10, and the maximum extraction was observed at pH 3. The results were confirmed again by optimizing the extraction between the pH range 2.5 to 3 and it is found that optimized extraction occurs at pH 2.7.

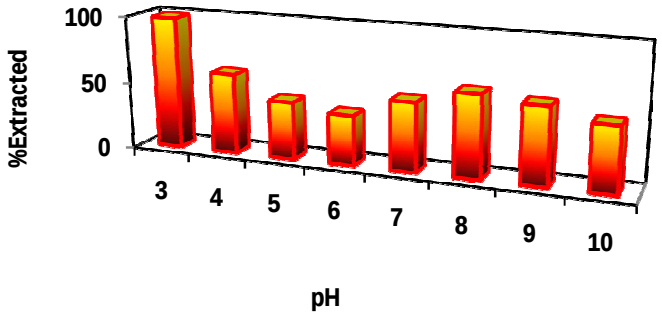

Figure 3. Percent extraction of Zn(II) ions by the HNPs at various pH.

Effect of Varying Analyte Concentration on the Sorption Capacity: Furthermore, at the optimized pH the effect of varying analyte concentration on the sorption capacity was tackled with various basic adsorption isotherms viz., Langmuir [32], Freundlich [33] and Temkin isotherm [34, 35]. The Langmuir adsorption isotherm plot for HNPs is shown in Figure 4.

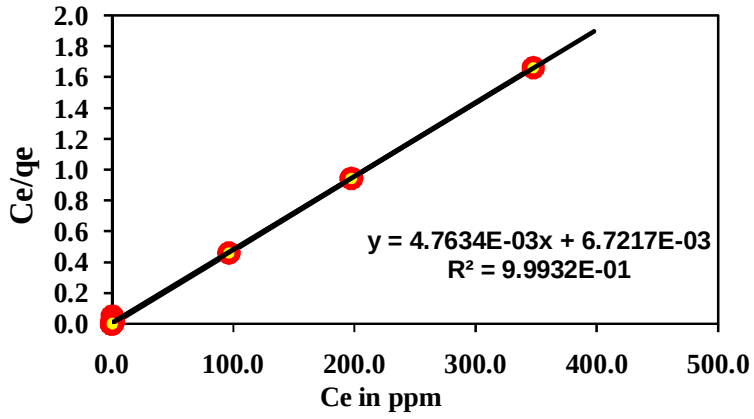

Figure 4. Langmuir adsorption isotherm

For Langmuir adsorption isotherm, the equation is,

$$\frac{C_e}{q_e} = \left(\frac{C_e}{Q_m}\right) + \left(\frac{1}{Q_b}\right) \qquad \text{---1}$$

Where, q_e: the amount of Zn(II) ions adsorbed per unit weight of sorbent at equilibrium concentration, b : the Langmuir constant related to affinity of binding sites (L mg^{-1}) and it is measure of energy of adsorption, Q_m : the maximum adsorption at monolayer (mg g^{-1}) and C_e : the equilibrium analyte concentration in mg L^{-1}. Accordingly, the maximum adsorption at monolayers (Q_m) for HNPs was computed to be 208.33 mg g^{-1}. Also, the values of Langmuir constants (b) were found to be 0.150 L mg^{-1}. These values were obtained from the slope and intercept of the linear plot of (C_e/q_e) against C_e. The R^2 vlue for regression is 0.9993. It indicates that our data fits in the model. Dimensionless equilibrium parameter, R_L which reveals the crucial individuality of the Langmuir adsorption isotherm is calculated by the equation (2) [36],

$$R_L = \left[\frac{1}{(1+bC_o)}\right] \qquad \text{---2}$$

Where, *b:* Langmuir constant, C_o: initial concentration of Zn(II) ions. The R_L values are calculated for HNPs and summarized in table 1, which are within the range of 0 to 1, representing favorable sorption of Zn(II) ions on HNPs.

Table 1. Computed R_L values for Zn(II) ion sorption

Concentration (ppm)	R_L for HNPs
1	0.583
2.5	0.358
5	0.218
12.5	0.100
25	0.053
37.5	0.036
50	0.027
75	0.018
100	0.014
150	0.009
250	0.006
400	0.003

The sorption capacity curves (Fig. 5) reveals that the maximum or equilibrium sorption capacity of the HNPs is 208 mg g^{-1}.

The linearized form of Freundlich adsorption equation dependent on sorption on a heterogeneous material is used along with its logarithmic form and given with equations (3) and (4),

$$q_e = K_F C_e^{1/n} \qquad \text{---3}$$

$$log\ q_e = log\ K_F + \left(\frac{1}{n}\right) log\ C_e \qquad \text{---4}$$

Where, K_F : Freundlich constant related to sorption capacity (mg g^{-1}),n : Freundlich constant related to adsorption intensity. Freundlich constants related to intensity (n) for HNPs was found 2.70 and the value of Freundlich constant related to sorption capacity (K_F) was found to be 92.737.The value of n obtained is in a range of 1 to 10 represents the potential of the HNPs as sorbents (Fig 6).

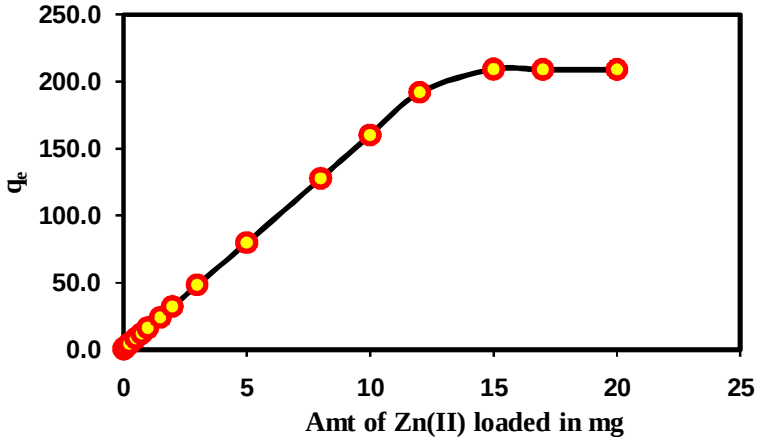

Figure 5. Sorption capacity curve for HNPs.

In addition, Freundlich adsorption isotherm is employed to the analytical data of HNPs (Fig. 6).

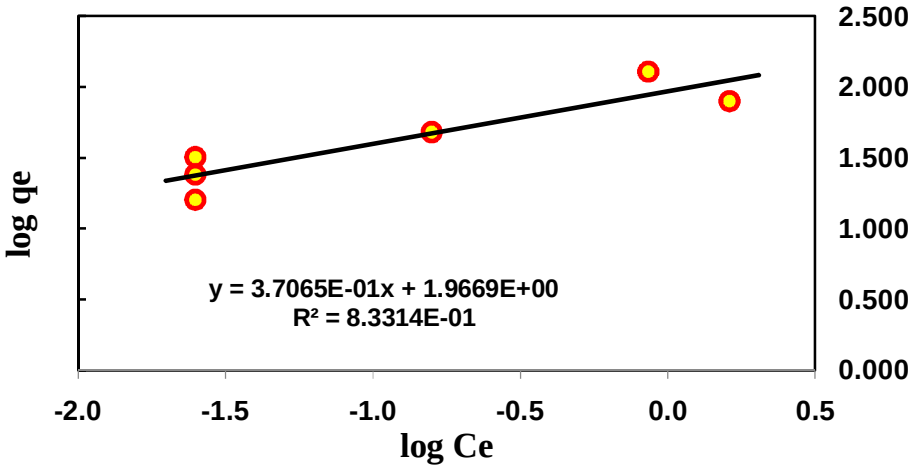

Figure 6. Freundlich adsorption isotherm for HNPs.

Along with the linear fitting, nonlinear fitting for Langmuir and Freundlich adsorption isotherms is also employed to the analytical data and the results were found in harmony with the Langmuir linear plot. The nonlinear fitting for Langmuir and Freundlich adsorption isotherms are given in Figure 7. The equation for non-linear fitting of Langmuir and Freundlich isotherm model is [37, 38],

$$q_e = \frac{Q_{max} \mathrm{b} C_e}{(1+\mathrm{b} C_e)} \qquad \text{---5}$$

Temkin adsorption isotherms for HNPs are plotted between *log* C_e versus q_e as shown in Figure 8**.** Its equation is depicted below,

$$q_e = (RT/b) log\ (AC_e) \qquad \text{---6}$$

Where, *b* : Temkin constant related to heat of sorption (J mol^{-1}), *R* : Gas Constant (8.314 J $mol^{-1}K^{-1}$), *T* : absolute temperature (25^{o}C or 298.15 *K*) and *A* : Temkin isotherm constant (Lg^{-1}). The linearized form of equation 6 is depicted as below,

$$q_e = B log A + B\ log C_e \qquad \text{---7}$$

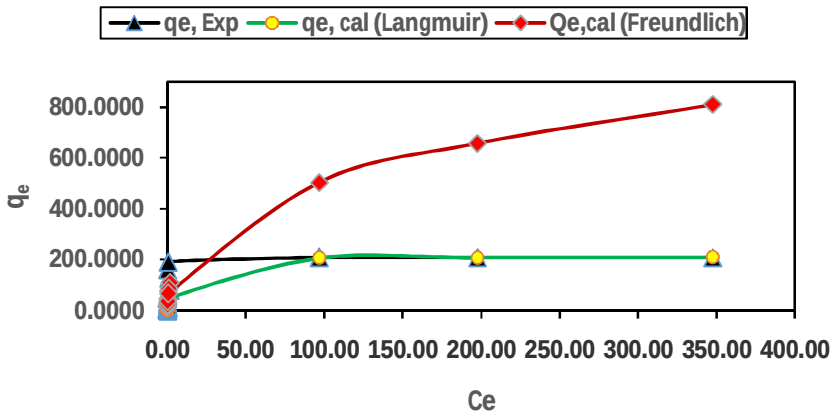

Figure 7. Nonlinear adsorption isotherms for HNPs.

Here, *B* : the slope from the plot. Temkin adsorption isotherm assumes that the heat of sorption reduces in a linear approach relatively than in logarithmic, as revealed from the Freundlich adsorption methodology. From the linearized Temkin equation the values of Temkin constant related to heat of sorption (*b)* and Temkin isotherm constant (*A*) is figured and found to be 0.397KJ mol^{-1}, and 1.78E+29 Lmg^{-1}. The higher R^2 value for Temkin adsorption isotherm model (R^2=0.9669) compared to the Freundlich adsorption isotherm (R^2=0.8331) assures that the decrease in heat of sorption is linear relatively than logarithmic.

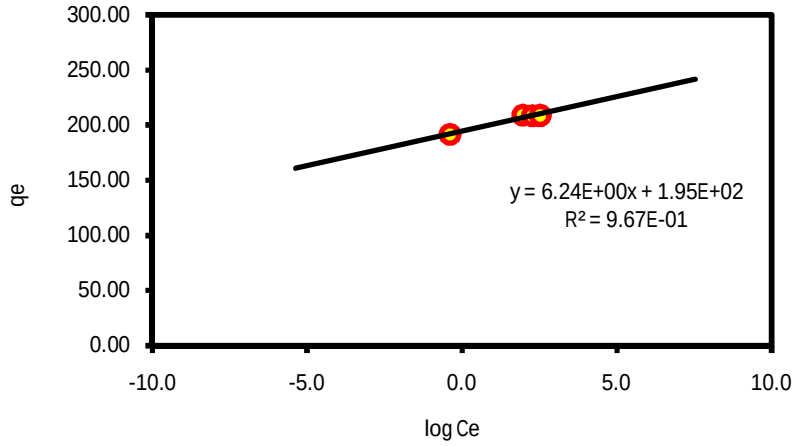

Figure 8. Temkin adsorption isotherm model.

Matrix Effect on Extraction of Zn(II) Ions: The method was applied to rodenticide residue analysis using HNPs. Commercial rodenticide samples containing approximately 3 % Zn_2P_3 corresponding to 90 mg elemental zinc were used for analyses to check the matrix effect on this method. Here, 0.118 g of rodenticide sample was dissolved to 100 mL, 1 mL aliquot subjected to extraction with 0.25 g HNPs by adjusting solution pH to 2.7. Then extracted zinc was stripped with 10 mL of 1 M HCl, and the sample was sequentially heated practically to dryness. Then it was further diluted to 10 mL with 1 M HNO_3 and used to determine the Zn(II) ion concentrations. Thus, the rodenticide samples were analyzed in triplicate with recovery of 100.00±0.36 %. Therefore, the quantitative recoveries with HNPs prove their successful application in real sample analysis without matrix interference and validate the method.

Comparison with Literature Reported Methods: The present method is compared with literature reports on preconcentrating of Zn(II) (table 2)

Table 2. Comparison of parameters derived from applied methodologies with hitherto reported literature for extraction of Zn(II) ions

Adsorbent	Adsorption Capacity (mg/g)	Reference
Bare Fe_3O_4@SiO_2	119	[39]
Amino-functionalized Fe_3O_4@SiO_2magnetic nano-adsorbent	169.5	[40]
Schiff's base adsorbed Fe_3O_4@SiO_2 nanoparticles	158	[41]
Macromolecule adsorbed Fe_3O_4@SiO_2 nanoparticles	208	Present work

APPLICATION

The synthesized hybrid iron oxide nanoparticles have been used for preconcentration and harmonious extraction of heavy metal ions from wastewaters.

CONCLUSIONS

It is concluded from the study that, the synthesized HNPs were successfully used for preconcentration of Zn(II) ions. The optimum operating factors like pH, utmost sorption capacity, are explored for preconcentration of Zn(II) ions. Subsequently, the effect of altering analyte concentrations was screened with basic adsorption models such as Langmuir, Freundlich and Temkin isotherms. The key HNPs were also successfully applied for preconcentration of Zn(II) ions in real sample (rodenticide residue) analysis without bare matrix interference. The sorbent has shown a significant adsorption capacity as compared to the methods reported in literature. So, these HNPs can be used for harmonious extraction of Zn(II) ions and in other requisite areas.

REFERENCES

[1]. Montes-Ga rcia, J.Perez-Juste, I. Pastoriza-Santos, L. M. LizMarzan., Metal Nanoparticles and Supramolecular Macrocycles: A Tale of Synergy, *Chem. Eur. J.*, **2014**, 20, 10874 – 10883.
[2]. Y.Yang, Y.Sun, N.Song, Switchable Host–Guest Systems on Surfaces, *Acc. Chem. Res.*, **2014**, 47, 1950-1960.
[3]. R. Chalasani., S.Vasudevan, Cyclodextrin-Functionalized Fe_3O_4@TiO_2: Reusable, Magnetic Nanoparticles for Photocatalytic Degradation of Endocrine-Disrupting Chemicals in Water Supplies, *ACS Nano*., **2013**, 7, 4093-4104.
[4]. S. Sayin, M.Yilmaz, Synthesis of A New Calixarene Derivative and Its Immobilization Onto Magnetic Nanoparticle Surfaces for Excellent Extractants Toward Cr(VI), As(V), and U(VI), *J. Chem. Eng. Data*, **2011**, 56, 2020-2029.
[5]. M.-M. Tian., D.-X. Chen, Y.-L. Sun, Y.-W. Yang, Q. Jia, Pillararene-functionalized Fe_3O_4 nanoparticles as magnetic solid-phase extraction adsorbent for pesticide residue analysis in beverage samples, *RSC Adv.*, **2013**, 3, 22111-22119.
[6]. S. Sayin, F. Ozcan, M. Yilmaz, Synthesis and evaluation of chromate and arsenate anions extraction ability of a N-methylglucamine derivative of calix[4]arene immobilized onto magnetic nanoparticles, *J. Hazard. Mater*, **2010**, 178, 312-319.
[7]. P. K. Mukherjee, Nanomaterials: Materials with immense potential, *J Applicable Chem*., **2016**, 5 (4), 714-718.
[8]. B. Zheng, M. Zhang, D. Xiao, Y. Jin, M.M.F. Choi, Fast Microwave Synthesis of Fe_3O_4 and Fe_3O_4/Ag Magnetic Nanoparticles Using Fe^{2+} as Precursor, *Neorganicheskie Materialy*, **2010**, 46, 1225–1230.
[9]. M. Mandal, S. Kundu, S.K. Ghosh, S. Panigrahi, T.K Sau, Magnetite Nanoparticles with Tunable Gold or Silver Shell, *Journal of Colloid and Interface Science*, **2005**, 286, 187–194.

[10]. N.Arsalani, H.Fattahi, M. Nazarpoor, Synthesis and Characterization of PVP-Functionalized Superparamagnetic Fe_3O_4 Nanoparticles as an MRI Contrast Agent, *Express Polymer Letters*, **2010**, 4, 329-338.
[11]. S. Chandra, M.D. Patel, H. Lang, D. Bahadur, Dendrimer-functionalized Magnetic Nanoparticles: A New Electrode Material for Electrochemical Energy Storage Devices, *Journal of Power Sources*, **2015**, 280, 217–226.
[12]. M.-M.Tian, D.-X. Chen, Y.-L. Sun, Y.-W. Yang, Q. Jia, Pillararene-Functionalized Fe3O4 Nanoparticles as Magnetic Solid-phase Extraction Adsorbent for Pesticide Residue Analysis in Beverage Samples, *RSC Adv.*,**201**3, 3, 22111–22119.
[13]. A. Alizadeh, M.M. Khodaei, M. Beygzadeh, D. Kordestani, M. Feyzi, Biguanide-Functionalized Fe_3O_4/SiO_2 Magnetic Nanoparticles: An Efficient Heterogeneous Organosuperbase Catalyst for Various Organic Transformations in Aqueous Media, Bull, *Korean Chem. Soc.*,**2012**, 33, 2546–2552.
[14]. P.C. Pinheiro, A.L. Daniel-da-Silva, D.S. Tavares, M. Pilar Calatayud, G.F Goya, T. Trindade, Fluorescent Magnetic Bioprobes by Surface Modification of Magnetite Nanoparticles, *Materials*, **2013**, 6, 3213–3225.
[15]. K. Turcheniuk, A.V. Tarasevich, V.P. Kukhar, R. Boukherroub, S. Szunerits, Recent Advances in Surface Chemistry Strategies for the Fabrication of Functional Iron Oxide Based Magnetic Particles, *Nanoscale*, **2013**, 5, 10729–10752.
[16]. B. Liu, M. Han, G. Guan, S. Wang, R. Liu, Z. Zhang, Highly-Controllable Molecular Imprinting at Superparamagnetic Iron Oxide Nanoparticles for Ultrafast Enrichment and Separation, *J. Phys. Chem. C.*, **2011**, 115, 17320–17327.
[17]. S. A. de Dios, M. E. Diaz-Garcia, Multifunctional Nanoparticles: Analytical Prospects, *Anal. Chim. Acta*,**2010**, 666, 1- 22.
[18]. X. Zhao, Y. Cai, T. Wang, Y. Shi, G. Jiang, Preparation of Alkanethiolate-Functionalized Core/Shell Fe3O4@Au Nanoparticles and its Interaction with Several Typical Target Molecules, *Anal. Chem.*,**2008**, 80, 9091–9096.
[19]. F. Girardi, E. Cappellett., J.Sandak, G. Bochicchio, B,Tessadri, S. Palanti, E. Feci, R. Di Maggio, Hybrid Organic–inorganic Materials as Coatings for Protecting Wood, *Prog. Org. Coat.*, **2014**, 77, 449-457.
[20]. Vandana Singh, Jadveer Singh and Preeti, Heterogeneous Fenton-Like Catalytic degradation of Remazol Brilliant Violet Dye Using Starch-Fe0Nps-Silica Composite, *J of Applicable Chem.*, **2017**, 6 (6), 1114-1129.
[21]. Y. P. He, S. Q. Wang, C. R. Li, Y.M. Miao, Z. Y. Wu, B. S. Zou, Synthesis and Characterization of Functionalized Silica-coated Fe_3O_4 Superparamagnetic Nanocrystals for Biological Applications, *J. Phys. D: Appl. Phys.*, **2005**, 38, 1342–1350.
[22]. R. D. Vernet, V. Boekelheide, Nuclear magnetic resonance spectroscopy. Ring-current effects on carbon-13 chemical shifts, *Proc. Nat. Acad. Sci. USA*, **1974**, 71, 2961-2964.
[23]. A. Rusen, M. A. Topcu, Investigation of zinc extraction from different leach residues by acid leaching, *Int. J. Environ. Sci. Technol.*,**2017**, doi:10.1007/s13762-017-1365-4.
[24]. B. Suryanarayana, V. Raghavendra, K. ChandraMouli, Structural, Electrical and Magnetic Properties of Ni0.5Zn0.5Fe_2O_4Nanoscale Particles by Co-Precipitation Method, J Applicable Chem., **2015**, 4 (4), 1237-1242.
[25]. Rahul R. Bhosale, Anand Kumar, Fares AlMomani, Ujjal Ghosh, Aliya Banu, Arwa Alahtem, Noor Naser, Nour Mardini, Deema Alhams, Afnan Alkhatib, Wadha Allenqawi, Amal Daifallah, Sol-Gel Synthesis of CoFe2O4/ZrO2 Nanoparticles: Effect of Addition of Proton Scavenger and Gel Aging Time, J Applicable Chem., **2016**, 5 (2), 384-392.
[26]. K. Tayade, S. Ingle, S. Attarde, Design, synthesis and characterization of a novel macrocycle/nanocrystal mesoporous hybrids, *International Journal of Advanced Scientific and Technical Research*, **2016**, 533-557.
[27]. Gusliani Eka Putri, Syukri Arief, Novesar Jamarun, Feni Rahayu Gusti, Adel Fisli, Zilfa, Upita Septiani, Synthesis and Microstructural Characterization of Modified Nano-Cerium Silica

Mesoporous by Surfactant-Assisted Hydrothermal Method, *J Applicable Chem.*,**2017**, 6 (6), 1058-1068.

[28]. P. Babji, I. Nageswara Rao and S. K. Das, Synthesis, Characterization and Antitumor activity of Fe2O3-Ag2O-TiO2 Nanocomposite on MCF-7 Human Breast Cancer Cells, *J Applicable Chem.*, **2015**, 4 (2), 550-556.

[29]. T. N. T. Phan, N. Louvard, S. A. Bachiri, J. Persello, A. Foissy, Adsorption of Zinc on Colloidal Silica, Triple Layer Modelization and Aggregation Data, *Colloids and Surfaces A*, **2004**, 244, 131–140.

[30]. M. Emadi, E. Shams, M. K. Amini, Removal of Zinc from Aqueous Solutions by Magnetite Silica Core-Shell Nanoparticles, *Journal of Chemistry*, **2013**: http://dx.doi.org/10.1155/ 2013 / 787682.

[31]. M. J. Goodall, S. A. Volz, J. J. Johnston Hurlbut D.B., R. E. Mauldin, D. L. Griffin, E. E. Petty, Determination of Zinc Phosphide Residues in Corn (*Zea mays*) Grain, Fodder, and Forage, Bull. *Environ. Contam. Toxicol*., **1998**, 60, 877–884.

[32]. I. Langmuir, The Adsorption of Gases on Plane Surface of Glass, Mica and Platinum, *The Research Laboratory of the General Electric Company*, **1918**, 1361.

[33]. H. Freundlich, Kapillarchemie: Eine Darstellung Der Chemie Der Kolloide and Verwanter Gebiete, *Academische Bibliothek, Leipzig, Germany*, **1909**, 1880.

[34]. M. I. Temkin, V. Pyzhev, Kinetics of Ammonia Synthesis on Promoted Iron Catalyst, *Acta Phys. Chim. USSR*, **1940**, 12, 327-356.

[35]. C. Aharoni, M. Ungarish, Kinetics of Activated Chemisorption. Part 2-Theoretical Models, *J. Chem. Soc. Faraday Trans.*, **1977**, 73, 456-464.

[36]. S. R. Tetgure, D. J. Garole, A. U. Borse, A. D. Sawant, Novel Extractant Impregnated Resin for Thorium Preconcentration from Different Environmental Samples: Column and Batch Study, *Separation Science and Technology*, **2015**, 50, 2496-2508.

[37]. I. Langmuir, The constitution and fundamental properties of solids and liquids, *J. Am. Chem. Soc.*,**1916**, 38, 2221–2295.

[38]. H. M. F. Freundlich, Uber die adsorption in losungen, *Zeitschrift fur Phys Chemie*, **1906**, 57, 385-470.

[39]. M. Emadi, E. Shams, M. K. Amini, Removal of Zinc from Aqueous Solutions by Magnetite Silica Core-Shell Nanoparticles, *Journal of Chemistry*, **2013**, http://dx. doi.org/10.1155/ 2013/ 787682.

[40]. S. Bao, L. Tang, K. Li, P. Ning, J. Peng, H. Guo, T. Zhu, Y. Liu, Highly selective removal of Zn(II) ion from hot-dip galvanizing pickling waste with amino-functionalized Fe_3O_4@SiO_2 magnetic nano-adsorbent, *Journal of Colloid and Interface Science*, **2016**, 462, 235-242.

[41]. K.C. Tayade, A.S. Kuwar, S.T. Ingle, S.B. Attarde, Synthesis of organic motif tailored hybrid nanoframes: Exploiting in vitro bioactivity and heavy metal ion extraction applications, *Materials Chemistry and Physics*, **2017**, 188, 8-17.